International Conference

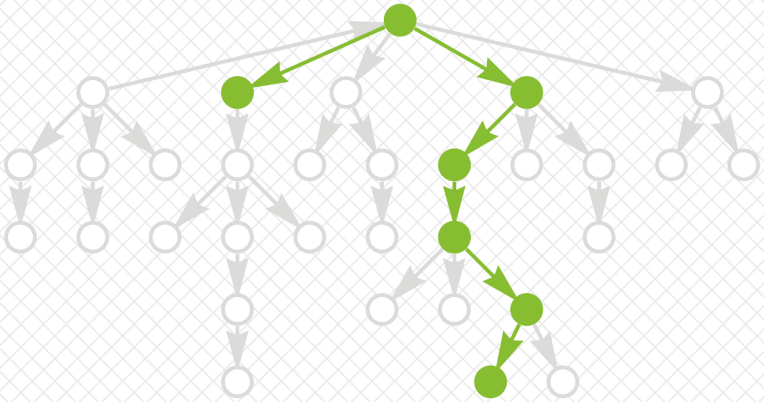

Instabilities and Control of Excitable Networks:

from macro- to nano-systems

Proceedings

Supporters and Sponsors

MIPT

Sk Skolkovo

RFBR RUSSIAN FOUNDATION FOR BASIC RESEARCH

COMS

BLOOD.RU

МОСКОВСКИЙ ЦЕНТР ТРАНСФЕРА ТЕХНОЛОГИЙ

Northern Biopharm Cluster

May 25-30, 2012
Dolgoprudny, Russia

www.icenet2012.net

Proceedings of the International Conference

Instabilities and Control of Excitable Networks:

From Macro- to Nano-Systems

Dolgoprudny, Russia

May 25-30, 2012

УДК 001:004.7:007.5:519.1:573:576.3:65.
ББК 28.071+28.91+32.97

Instabilities and Control of Excitable Networks / Moscow: MAKS-Pess, 2012, 133 p.

The present book contains the proceedings of the International Conference "Instabilities and Control of Excitable Networks: From Macro- to Nano-Systems" (ICENet-2012) hosted by Moscow Institute of Physics and Technology in Dolgoprudny, Russia, on 25-30 May, 2012. The conference was devoted to the problems of complex excitable network dynamics in physiology, biomedicine, physics, chemistry and social systems.

Неустойчивости в возбудимых сетях и возможности управления ими / Москва: МАКС-Пресс, 2012. — 133 с.

В сборник вошли труды участников международной конференции "Instabilities and Control in Excitable Networks: From Macro- to Nano-Systems" (Неустойчивости в возбудимых сетях и возможности управления ими: от макро- к нано-системам), проходившей в Московском физико-техническом институте (г. Долгопрудный, Россия) в период с 25 по 30 мая 2012. Конференция была посвящена изучению сложного возбудимого динамического поведения систем, организованных по сетевому принципу, в физиологии, биомедицине, физике, химии и социальной сфере.

Threshold activation of intravascular fibrin polymerization and gel formation under intensive blood flow conditions. Theoretical analysis.

A.S. Rukhlenko[1,*], K.E. Zlobina[2] and G.Th. Guria[1,2]

[1]*Moscow Institute of Physics and Technology, Dolgoprudny, Russia*
[2]*National Research Centre for Haematology, Moscow, Russia*
[*]*e-mail address: aleksey.rukhlenko@gmail.com*

1 Introduction

It is commonly accepted that platelets as well as serine proteases participating in biochemical reactions of fibrin production play an essential role in the development of intravascular blood coagulation [1–3]. At the same time, in the initiation of intravascular blood coagulation an important role belongs to the condition of vessel walls (including their impairment by ulcers or sclerosis and the state of endothelium) [4–9].

According to current scientific views, the initiation of the intravascular coagulation processes may occur either as a result of the disruption of vessel wall barrier properties [5, 10, 11], or due to the activation of platelets in the shear flows (mainly near the vessel wall) where the shear rate exceeds $\sim 5400\ s^{-1}$ [12–14].

Within the scope of this work, we focus only on the situations of blood flow in which shear rate does not exceed $\sim 10^3\ s^{-1}$. Therefore, hydrodynamical activation of platelets will not be taken into consideration in this research.

Main attention will be paid to intravascular coagulation initiated by procoagulants that infiltrate into the blood flow when endothelium barrier properties are diminished due to the intensification of wall shear stress [15–18].

Within the approach suggested, the permeability of endothelium layer will be assumed to depend on the wall shear stress in a threshold manner. The highest stresses in blood vessels normally occur in the areas of greater stenosis narrowing, which appear, for instance, due to the local formation of atherosclerotic plaques. This is precisely the reason why the starting centers of above-threshold stimulation of thrombus formation are usually associated with the location of atherosclerotic plaques in the vessels [15–18].

The role of pro-coagulant factors that enter blood flow from atherosclerotic plaques is mostly performed by the products of inflammatory processes that take place in the plaques [19, 20]. Regardless of procoagulant's biochemical nature, we consider all substances of that type as pro-coagulants in cases when they can serve as primary activators of blood coagulation [21, 22].

The threshold activation of the blood coagulation system (BCS) cascade of reactions manifests itself by means of a self-accelerated production in the blood flow of a range of key biochemical agents — serine proteinases (factors IIa (thrombin), Xa, VIIIa, Va etc.), among which the central role is played by thrombin. In this work, thrombin generation and its distribution in the vessel was taken into consideration within scope of phenomenological model [21–25]. The biological significance of thrombin is dealt with its catalytic ability to

convert fibrinogen molecules (present in the blood in inactive form) into fibrin-monomers capable of fast precipitous polymerization.

The formation of a fibrin polymer network in the blood flow can change the flow pattern even up to complete stoppage of blood flow.

The main aim of this work was to develop a description of the mass transfer processes involving the formation of fibrin thrombi in vessels having variable crosssection of the lumen. The study of the revelant problems within the framework of the suggested approach allowed us to reveal several typical scenarios of intravascular clot formation, as well as to build parametrical diagrams of the blood liquid state stability in intense flows.

The results obtained probably have some value in the discussion of indications for stenting procedures practically used for the vessel remodeling in patients.

2 Model description

2.1 Geometry

Blood vessel with stenosis (atherosclerotic plaque) on its lower wall was considered in a two-dimensional approximation (see fig. 1). Vessel walls were supposed to be rigid.

The form of stenosed vessel wall was approximated by formula:

$$f(x) = L_y(1-s)e^{-\frac{x^2}{2d^2}}, \tag{1}$$

where L_y denotes vessel width, H denotes vessel minimal width, $s = (H/L_y) \in (0;1)$ reflects relative size of minimal lumen, and d corresponds to stenosis width (see fig. 1).

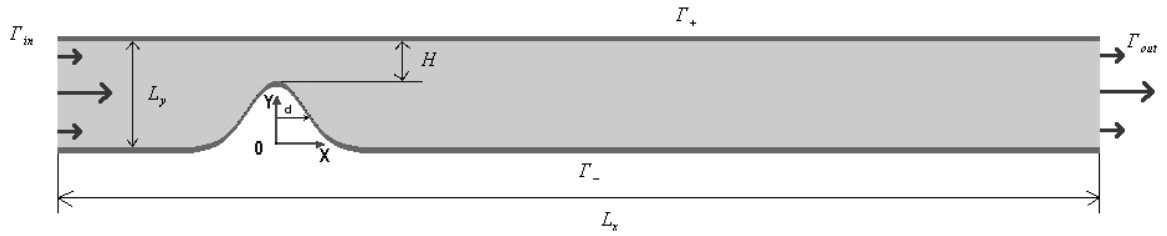

Figure 1: Vessel's fragment geometry. L_x, L_y and H correspond to vessel length, width and minimal vessel width. Γ_+ and Γ_- refer to upper and lower vessel walls respectively. Γ_{in} and Γ_{out} denote inlet and outlet boundaries respectively.

2.2 Governing equations

Blood was supposed to be a Newtonian fluid with viscosity ν and density ρ. Hemodynamics was described by means of modified Navier-Stokes equations:

$$\frac{\partial \vec{V}}{\partial t} + \left(\vec{V}, \vec{\nabla}\right)\vec{V} = -\frac{1}{\rho}\vec{\nabla}\, p + \nu\nabla^2\vec{V} - \alpha_p(M_1, M_2)\nu\vec{V} \tag{2}$$

$$\left(\vec{\nabla}, \vec{V}\right) = 0, \tag{3}$$

where t denotes time, $\vec{\nabla}$ is well-known Hamilton's operator, $\alpha_p(M_1, M_2)$ describes filtration resistance of fibrin polymer network (in case it is formed), M_1 and M_2 refer to statistical moments of fibrin polydisperse system (see below)[1].

[1]The polymer structure formed was considered as a porous media with a specific (non-constant) Darcy coefficient. The value of Darcy coefficient depended on the state of polydisperse macromolecule fibrin system.

The kinetics of blood coagulation reactions was described in the framework of the phenomenological model [21–24]:

$$\frac{\partial u}{\partial t} = -k_d u - \nabla\cdot\left(\vec{V}u - D_u\nabla u\right) \tag{4}$$

$$\frac{\partial \theta}{\partial t} = k_u u + \frac{\alpha\theta^2}{\theta+\theta_0} - \chi_1\theta - \gamma\theta\varphi - \nabla\cdot\left(\vec{V}\theta - D_\theta\nabla\theta\right) \tag{5}$$

$$\frac{\partial \varphi}{\partial t} = \beta\theta\left(1-\frac{\varphi}{c}\right)\left(1+\left(\frac{\varphi}{\varphi_0}\right)^2\right) - \chi_2\varphi - \nabla\cdot\left(\vec{V}\varphi - D_\varphi\nabla\varphi\right) \tag{6}$$

$$\frac{\partial F_g}{\partial t} = -k_g F_g\theta - \varepsilon_g\left(F_g - F_g^0\right) - \nabla\cdot\left(\vec{V}F_g - D_g\nabla F_g\right) \tag{7}$$

$$\frac{\partial M_1}{\partial t} = k_g F_g\theta - k_r M_1 - \nabla\cdot\left(b_p\vec{V}M_1 - D_f\nabla M_1\right) \tag{8}$$

$$\frac{\partial M_2}{\partial t} = k_g F_g\theta + 4k_p(M_2+M_1)^2 - \frac{k_b}{3}\left(\frac{M_2^2}{M_1} - M_1\right) - k_r M_2 - \nabla\cdot\left(b_p\vec{V}M_2 - D_f\nabla M_2\right), \tag{9}$$

where u denotes the concentration of the primary activator of blood coagulation, θ and φ denote concentrations of the activator (thrombin) and the inhibitor of biochemical network of blood coagulation reactions (see [26, 27] and [21]), F_g corresponds to fibrinogen (fibrin precursor) concentration. M_1 and M_2 are first and second fibrin moments that are defined through the concentration of k-meres of fibrin F_k as [21]:

$$M_n = \sum_{k=1}^{\infty} k^n F_k, \;\; n = 1,\, 2. \tag{10}$$

It is well-known that M_1 reflects the total amount of fibrin-monomer molecules in all polymerized and unpolymerized forms in the considered element of volume, while the ratio M_2/M_1 determines weight-averaged molecular weight [28, 29] M_w of fibrin polymer molecules in the system considered [30]:

$$M_w = \sum_{k=1}^{\infty} m_0 k\cdot w_k = m_0\frac{M_2}{M_1}, \tag{11}$$

where m_0 denotes the molecular weight of fibrin-monomer and $w_k = {}^{kF_k}\Big/\left(\sum\limits_{m=1}^{\infty} mF_m\right)$ corresponds to the weight fraction of k-meres in the system. The weight-averaged number of fibrin-monomers in polymer molecules of fibrin N_w could be expressed as:

$$N_w = \frac{M_w}{m_0} = \frac{M_2}{M_1}. \tag{12}$$

We assumed that with the increase in the polymer chains length they will become less and less transportable by the flow. To take into account this circumstance, a special term b_p has been introduced into equations (8)-(9) as a coefficient of polymer chains transport by the flow (see [23–25] for details).

We believe that the system equations (2)-(9) can correctly describe the early stages of intravascular coagulation processes, that is, the situations in which the loss of stability of the blood liquid state triggers the bulk chain processes of generation of fibrin-monomer molecules followed by their polymerization. The dynamics of fibrin-polymer microemboli formation has several stages [31, 32]. The early stage, nucleation, is followed by the stage

of emboli growth up to the size comparable to the mean distance between them. Next comes the stage when neighbouring fibrin-polymer clots start to overlap, that is, an essential interaction between them is established. During later stages, the system evolution results in gel formation in the vessel under consideration.

In this work, it will be assumed that during all the listed stages of coagulation the blood density undergoes no changes. Unlike the density, the kinetic coefficients ν, α_p, D_f and b_p undergo an essential change during the stage-to-stage transition. It was assumed that during the fibrin-polymer clots nucleation the value of blood viscosity ν is equal to the initial value, the filtration resistance α_p is taken to be negligibly small, and the coefficient of polymer chains transport by the flow b_p and the diffusion coefficient D_f are adequately represented by the expressions:

$$b_p = 1 \tag{13}$$

$$D_f = D/N_w \tag{14}$$

where D is the fibrin-monomer diffusion coefficient.

When the growing polymer clusters begin to mutually overlap, the process is commonly termed as the formation of a semi-diluted polymer solution [33, 34]. The following inequation serves as a criterion of a semi-diluted polymer solution formation:

$$N_w \geq N_w^s \tag{15}$$

where N_w^s is the weight-averaged number of fibrin monomer molecules in polymer coils at the appearance of semi-diluted conditions.

Fulfillment of these conditions actually implies that functional dependences of the listed coefficients ν, α_p, D_f and b_p on statistical moments M_1 and M_2 begin to change.

In the present work, the description of the dependences of the kinetic coefficient s on the moments of the distribution of a fibrin moleculae polydispersional system employed asymptotic expressions that in the limitary cases turn into well-known in polymer physics expressions. The actual form of the respective dependences is given below (see [23–25] for details):

$$\alpha_p = k_{num} N_a^2 M_1^2 K^2 l_0^4 \cdot (1 - b_p) \tag{16}$$

$$D_f = D \cdot \frac{1}{N_w} \cdot \frac{1}{1 + N_w/N_w^s} \tag{17}$$

$$b_p = \frac{1}{1 + N_w/N_w^s} \tag{18}$$

where N_a is the Avogadro number, $k_{num} = 10^{-24}\ mole^2/(nM^2 \cdot cm^6)$ is the coefficient for the conversion of length dimensions.

The work mainly focused on the early stages of fibrin gel formation in the blood flow. Therefore it was assumed that when the mean length of polymer chains N_w exceeds the characteristic value of the half-dilution condition N_w^s by two or more orders ($N_w = 10^2 \cdot N_w^s$), a sufficiently "mature" gel is formed, and the research of its further evolution remains outside the scope of this work's objectives[2]

[2]It should be noted that adopting of this assumption lets to avoid us analysis of the singular solutions of equations, describing the dynamics of statistical moments M_1 and M_2, i.e. the situations when M_2 blows up [35].

2.3 Boundary and initial conditions

Poiseuille's conditions were applied at the left boundary of the considered area Γ_{in}:

$$V_x|_{\Gamma_{in}} = \frac{4V_0}{L_y^2} y(L_y - y) \tag{19}$$

$$V_y|_{\Gamma_{in}} = 0 \tag{20}$$

Pressure on the outlet boundary was assumed to be equal to zero:

$$p|_{\Gamma_{out}} = 0 \tag{21}$$

The no-slip conditions were satisfied at the boundaries Γ_+ and Γ_-.

The values of u, θ, φ, M_1 and M_2 on Γ_{in} were supposed to be equal to zero, while F_g concentration on Γ_{in} was assumed to be equal to initial fibrinogen concentration F_g^0. On the vessel outlet Γ_{out} the zero-gradient conditions were used for all chemicals.

Vessel walls were supposed to be impermeable for all chemicals but the primary activator. This means that for θ, φ, F_g, M_1 and M_2 the zero-gradient boundary conditions were set on Γ_+ and Γ_-. The upper (non-stenosed) vessel was supposed to be impermeable for u. To describe the process of primary activator infiltration into the blood flow through the lower (stenosed) vessel wall the following boundary condition was used for u on Γ_-:

$$-D \left.\frac{\partial u}{\partial \vec{n}}\right|_{\Gamma_-} = \mu(|\gamma_{sh}|)\left(u_0 - u|_{\Gamma_-}\right) \tag{22}$$

where operator $\left.\frac{\partial}{\partial \vec{n}}\right|_{\Gamma_-}$ denotes the space derivative normal to Γ_-, u_0 denotes primary activator concentration under the vessel wall, and $u|_{\Gamma_-}$ corresponds to the concentration of primary activator in the blood flow near the lower vessel wall (Γ_-).

Table 1: Parameter values

Parameter	Value	Refs.	Parameter	Value	Refs.
α	$3.33\cdot10^{-2}\ s^{-1}$	[21, 22]	k_b	$1.67\cdot10^{-3}\ s^{-1}$	[21, 22]
θ_0	$5\ nM$	[21, 22]	n_0	$10^{10}\ cm^{-3}$	[36]
χ_1	$8.33\cdot10^{-4}\ s^{-1}$	[21, 22]	F_g^0	$9\cdot10^3\ nM$	[21, 22]
γ	$8.33\cdot10^{-2}\ (nM\cdot s)^{-1}$	[21, 22]	D_u	$3\cdot10^{-7}\ cm^2/s$	[21, 22]
β	$2.5\cdot10^{-5}\ s^{-1}$	[21, 22]	D_φ	$3\cdot10^{-7}\ cm^2/s$	[21, 22]
c	$5\ nM$	[21, 22]	D_θ	$3\cdot10^{-7}\ cm^2/s$	[21, 22]
ε_g	$1.66\cdot10^{-6}\ s^{-1}$	[21, 22]	D_g	$3\cdot10^{-7}\ cm^2/s$	[21, 22]
φ_0	$0.05\ nM$	[21, 22]	D	$3\cdot10^{-7}\ cm^2/s$	[21, 22]
χ_2	$0.35\ nM$	[21, 22]	k_d	$1.66\cdot10^{-6}\ s^{-1}$	[21, 22]
k_g	$5\cdot10^{-6}\ (nM\cdot s)^{-1}$	[21, 22]	k_u	$1.66\cdot10^{1}\ s^{-1}$	[21, 22]
k_p	$2.5\cdot10^{-4}\ (nM\cdot s)^{-1}$	[21, 22]	k_r	$1.67\cdot10^{-2}\ s^{-1}$	[21, 22]
γ_1	$10\ dyn/cm^2$	[15, 16, 18]	μ_1	$2\cdot10^{-12}\ cm/s$	[23, 24]
γ_2	$20\ dyn/cm^2$	[15, 16, 18]	u_0	$100\ nM$	[23, 24]
ν	$5\cdot10^{-2}\ cm^2/s$	[36]	ρ	$1\ g/cm^3$	[36]
L_x	$7.5\ cm$		L_y	$1\ cm$	
K	10	[37]	l_0	$1.5\cdot10^{-6}\ cm$	[37, 38]
N_a	$6.02\cdot10^{23}\ mol^{-1}$				

The permeability μ of the lower vessel wall Γ_- depended on wall shear stress γ_{sh} in a piecewise-linear manner:

$$\mu = \begin{cases} \mu_1, & |\gamma_{sh}| \le \gamma_1 \\ \dfrac{|\gamma_{sh}| - \gamma_1}{\gamma_2 - \gamma_1}(\mu_2 - \mu_1) + \mu_1, & \gamma_1 < |\gamma_{sh}| < \gamma_2 \\ \mu_2, & |\gamma_{sh}| \ge \gamma_2 \end{cases}, \tag{23}$$

where μ_1 denotes the permeability of vessel wall for sub-threshold wall shear stress values, and μ_2 corresponds to the permeability for over-threshold ones.

At the initial moment $t = 0$ all variables but F_g were assumed to be equal to zero in the interior part of calculation domain while F_g was assumed to be equal to F_g^0. The $\vec{V}$ and p fields were assumed to be equal to their stationary values in the given boundary conditions (i.e. stationary flow).

The values of all parameters used in numerical calculations are presented in the Table 1 (see [23, 24]).

3 Results

3.1 Early stages of thrombi formation processes. Typical scenarios

Numerical simulation of the model described above opened the possibility to calculate spatio-temporal distribution of M_1, M_2, N_w, etc[3]. in the vessel. Some scenarios are shown in figures 2, 3 and 4. The gray color scale at these figures represents weight-average number of fibrin monomers in polymer chains N_w (see eqn. (12)). The maximum of the scale (white color) is N_w^s (see eqn. (15))[4]. This means that white color represents clots while grey shades represent microthrombi with different lengths of polymer chains.

There is a recirculation zone behind the atherosclerotic plaque in all investigated scenarios (see figures 2, 3 and 4). In the present work only the thrombus formation events taking place in recirculation zone were investigated. Within the scope of the presented approach we found 3 typical scenarios of thrombus formation events. In scenarios 1 and 2, a solid massive thrombus is formed as the result of blood coagulation system activation (see figures 2d and 3d). In contrast, the result of the activation of coagulation system in scenario 3 is a floating friable structure without a sharp border (see fig. 4c). It can be seen from fig. 4c, the floating structure has a long "tail" of mircothrombi clouds downstream.

Numerical simulations have shown that in all scenarios early stages of coagulation processes development are the same. The nucleation of a macroscopic thrombus always happens in the region of reattachment point (see figures 2a, 3a and 4a). Then the stage of macroscopic fibre-like structure formation comes (see figures 2b, 3b and 4b). The direction of the growth of the fibre-like structure is determined by the separatrix line, which divides the core of the flow from the recirculation zone.

After that, there are three possible types of system behavior depending on the parameter values:

- fibre structure successively thickens (see fig. 2c) and a solid thrombus is formed in the recirculation zone (see fig. 2d);
- after some time of fibre structure growth the gelation front splitting happens (see fig. 3c) and solid thrombus in the recirculation zone is formed (see fig. 3d) as a result of a two-side clot growth;

[3] Numerical methods, used in analysis of presented model are described in [23–25].

[4] Note that N_w can be greater than N_w^s.

- formation of a floating friable structure takes place (see fig. 4c).

3.2 Threshold-like activation of thrombus formation process

Numerical simulations not only revealed the typical patterns of blood clot formation, but also allowed us to build parametric diagrams of blood liquid state stability. Using our mathematical model we investigated the influence of blood flow rate, vessel wall permeability and the shape of atherosclerotic plaque on threshold activation of blood coagulation processes.

Blood flow rate is characterized by a dimensionless parameter — Reynolds number:

$$Re = \frac{V_0 L_y}{\nu} \tag{24}$$

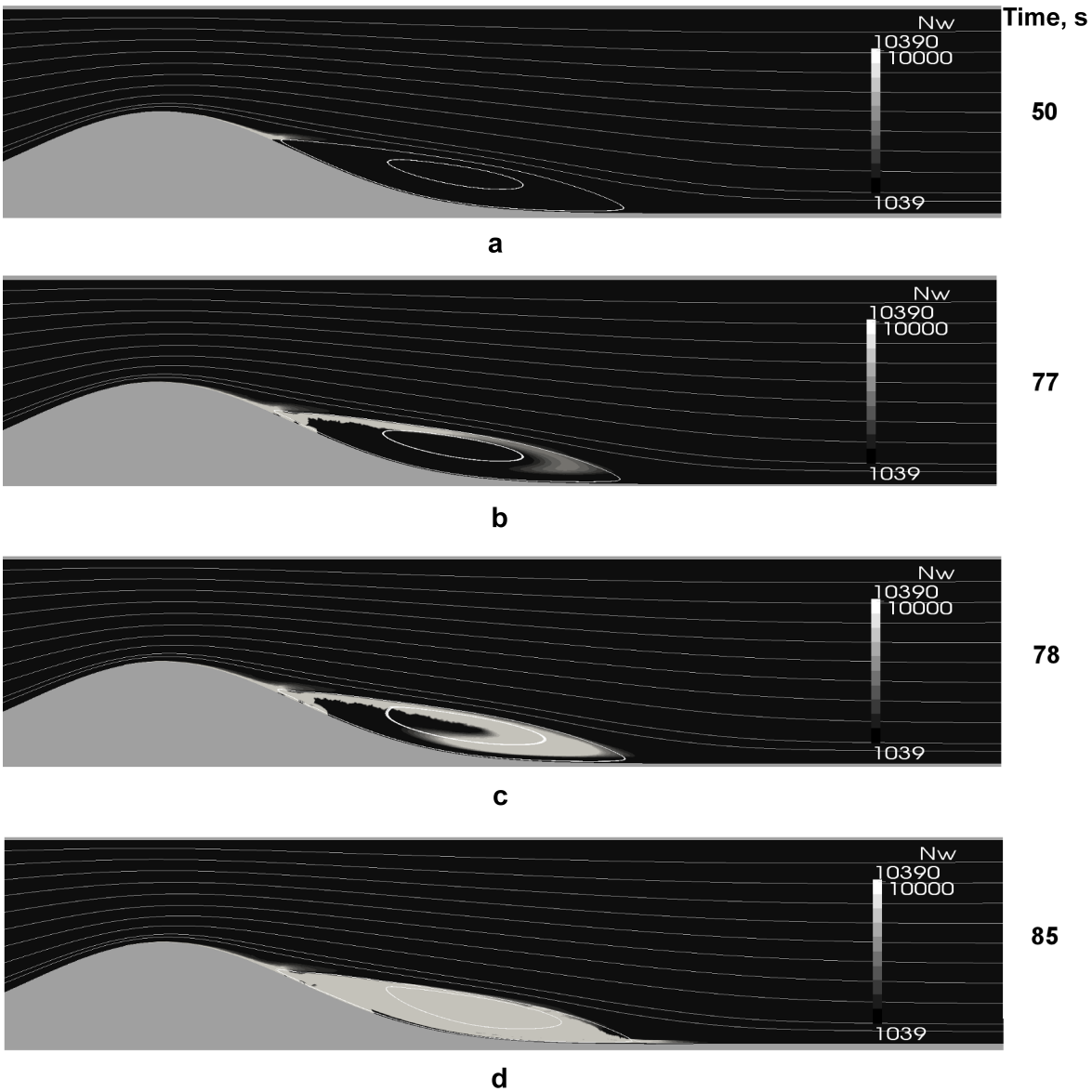

Figure 2: Scenario 1, solid thrombus formation through 1-side gelation front. Gray-scale map of N_w distribution in the vessel, white areas are places of fibrin gel formation ($N_w \geq N_w^{pol}$). a-d are successive stages of the process: a — thrombus nucleation, b — formation of fibre-like fibrin structure, c — fibre-like structure thickening, d — solid thrombus. $Re = 130$, $s = 0.5$, $\tilde{d} = 0.5$, $\tilde{\mu}_2 = 9.5$.

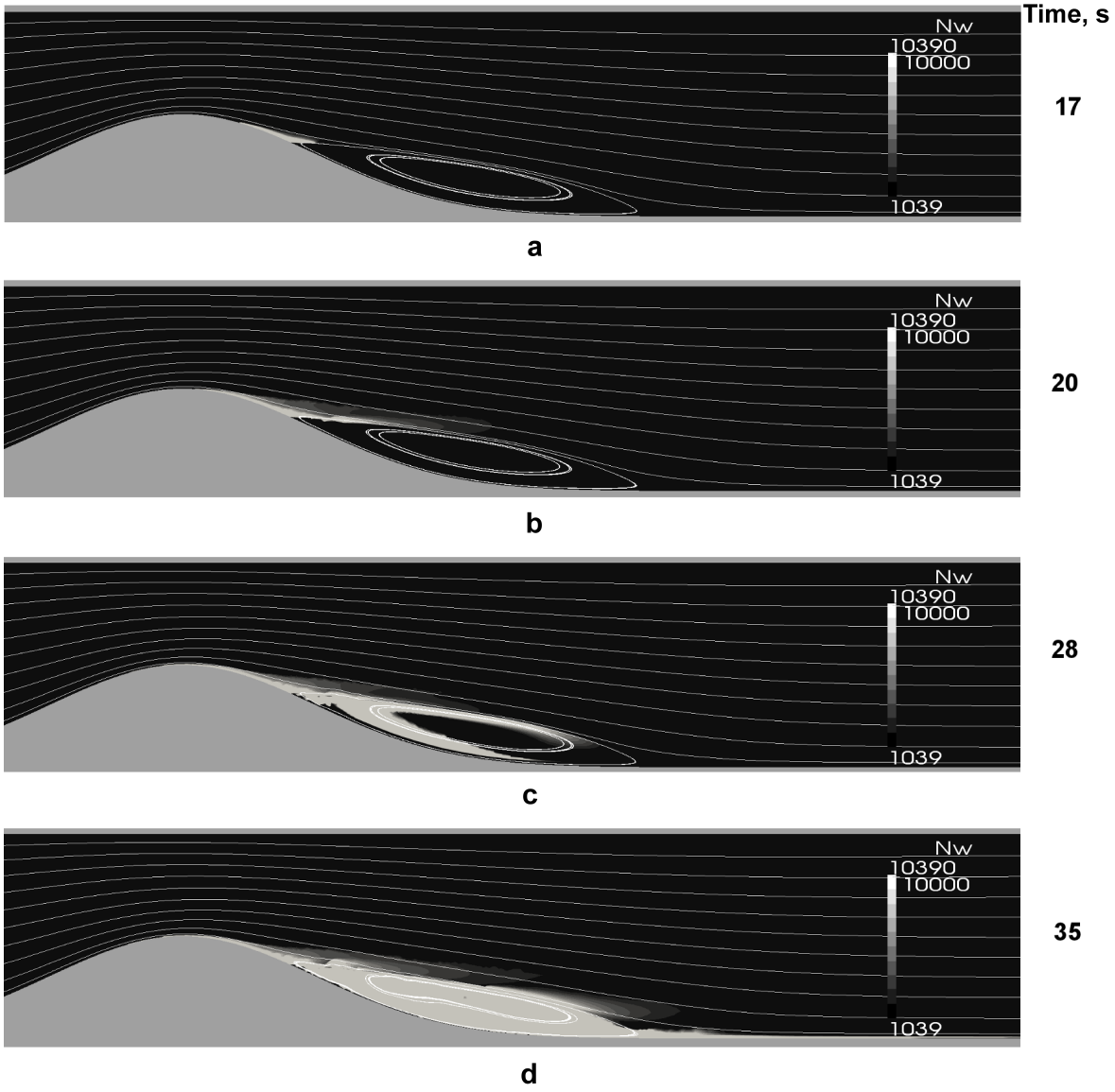

Figure 3: Scenario 2, solid thrombus formation through 2-side gelation front. Gray-scale map of N_w distribution in the vessel, white areas are the places of fibrin gel formation ($N_w \geq N_w^{pol}$). a-d are successive stages of the process: a — thrombus nucleation, b — formation of fibre-like fibrin structure, c — two-side gelation front, d — solid thrombus. $Re = 130$, $s = 0.5$, $\tilde{d} = 0.5$, $\tilde{\mu}_2 = 95$.

Vessel wall permeability may be characterized by dimensionless maximal vessel wall permeability:

$$\tilde{\mu}_2 = \mu_2 u_0 \cdot \frac{k_u}{L_y(\alpha - \chi_1)^2 \theta_0} \tag{25}$$

The parametric diagram of blood coagulation system regimes is presented in fig. 5. Parametric plane $(Re, \tilde{\mu}_2)$ is divided in two main zones denoted as "I" and "II". When the representative point is located in zone "I" the system evolves to stationary state with $N_w < N_w^{pol}$. This means that only formation of micro-thrombi (see [22]) takes place in the system. When the representative point is located in zone "II" N_w reaches and exceeds N_w^{pol} at some moment of time, that means that fibrin gelation, i.e. formation of macroscopic thrombi, occurs.

Figure 5 shows that the region where thrombus formation starts has a form of a "tongue"

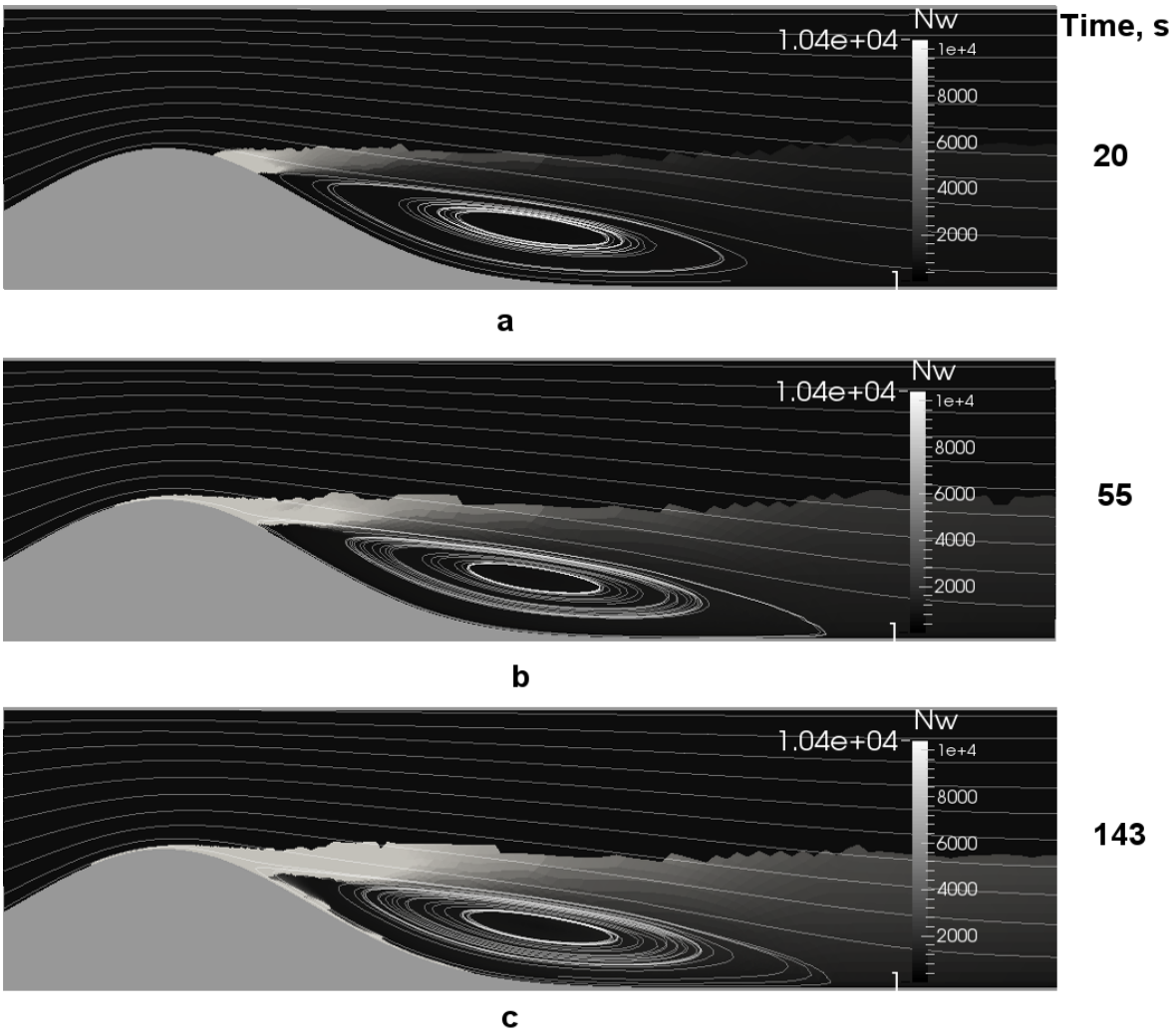

Figure 4: Scenario 3, floating fibrin structure formation. Gray-scale map of N_w distribution in the vessel, white areas are the places of fibrin gel formation ($N_w \geq N_w^{pol}$). a-c are successive stages of the process: a — thrombus nucleation, b — formation of fibre-like fibrin structure, c — thick and friable floating fibrin structure. $Re = 200$, $s = 0.5$, $\tilde{d} = 0.5$, $\tilde{\mu}_2 = 9.5$.

and that the range of Reynolds number values where it happens is limited both above and below. For any $\tilde{\mu}_2 > \tilde{\mu}_2^{min}$ two thresholds of hydrodynamic activation of blood coagulation exist.

For example, if we follow the horizontal line with arrows in figure 5, the first threshold is at $Re = Re_1$: if $Re < Re_1$, the value of wall shear stress is less than γ_1 and primary activator u doesn't appear in blood flow; otherwise fibrin clot is formed. The second threshold is at $Re = Re_2$: if $Re > Re_2$, convective flow washes coagulation substances away, otherwise thrombus formation starts.

This means that both increasing and decreasing of blood flow intensity may lead to thrombi formation, depending upon initial conditions.

In figure 5 one can see a vertical line $Re = Re_{\gamma_2}$. This value of Reynolds number corresponds to wall shear stress equal to γ_2 that means that vessel wall permeability $\mu = \mu_2$ (see eqn. (23)). In other words, it is the intensity of blood flow that leads to the plaque rupture.

Some part of zone "I" is on the right side of $Re = Re_{\gamma_2}$ in fig. 5, that means that in spite of plaque rupture thrombi formation doesn't occur. This type of system behavior may be

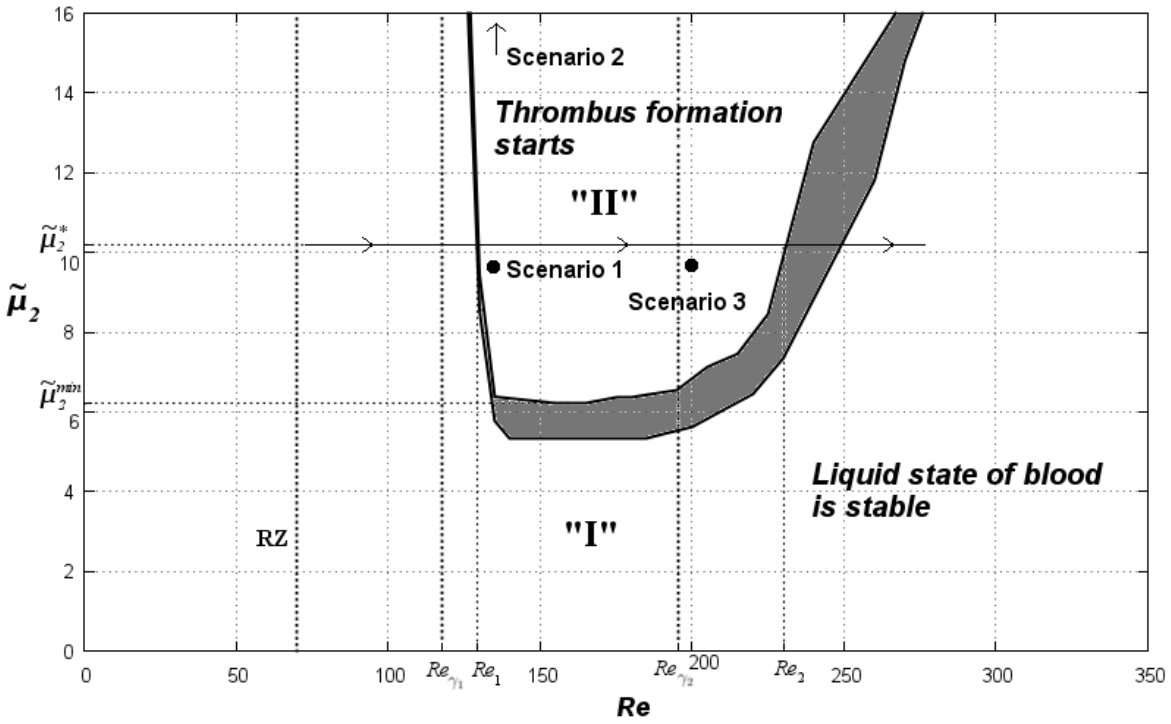

Figure 5: Parametric diagram of blood coagulation system regimes. This diagram describes the influence of the vessel wall permeability $\tilde{\mu}_2$ and blood flow rate Re on thrombi formation threshold. Grey ribbon between zones "I" and "II" is a region where it is difficult to detect whether the point belongs to zone "I" or "II". Parameter values: $s = 0.5$, $\tilde{d} = 0.5$.

associated with asymptotic plaque rupture [39, 40].

It was found that in the vicinity of the border between zones "I" and "II" the following scaling law is valid for the nucleation time T^* (given constant Re):

$$(\tilde{\mu}_2 - \tilde{\mu}_2^{crit}) T^{*\,3} = C_1 = const, \tag{26}$$

where $\tilde{\mu}_2^{crit}$ is specific value of $\tilde{\mu}_2$, located in the "grey" area (see fig. 5), and C_1 is a value independent on $\tilde{\mu}_2$.

It was also shown that in the vicinity of the left border of zone "II" the following scaling law is valid (given constant $\tilde{\mu}_2$):

$$(Re - Re_{crit}) T^{*\,3} = C_2 = const \tag{27}$$

where Re_{crit} is the specific value of Re, located in the "grey" area (see fig. 5), and C_2 is the value independent on Reynolds number (Re).

In other words, it appeared that in the vicinity of the liquid state stability border the clot nucleation time grows up to infinity (see (26)-(27)). This result can be compared with the results of the theory of first-order transitions, where similar scaling laws connecting the extent of supersaturation with the nucleation time exist [41, 42].

To investigate the influence of stenosis shape on blood coagulation threshold the $(s, Re, \tilde{d})$ parametric plane was scanned (see fig. 6), given the constant $\tilde{\mu}_2$. The dimensionless parameter $\tilde{d}$ characterizes the width of the atherosclerotic plaque:

$$\tilde{d} = d / L_y \tag{28}$$

It appeared that the surface dividing the sub- and superthreshold regimes of blood coagulation system is saddle-like. For a chosen value of $\tilde{\mu}_2$ the section of this surface by the $\tilde{d} = 0.4$ plane crosses the saddle-point (see fig. 6b). It can be clearly seen that the Reynolds number range where macroscopic thrombus formation takes place for $0.2 < s < 0.4$ is significantly wider than for $0.6 < s < 0.8$.

4 Discussion

In this work the blood coagulation system hydrodynamical activation conditions and the characteristic scenarios of the early stages of thrombi formation processes in stenosed vessels were investigated. Intravascular activation of blood coagulation processes was assumed to be caused by primary pro-coagulants that infiltrated into the blood flow through the vessel wall from adjacent tissues.

Clearly, the mathematical description of intravascular blood coagulation processes was oversimplified in the present work. The model suggested only took into consideration the biochemical part of the haemostasis system. It was taken into account that the processes of the hydrodynamical activation of the platelet-based part of the haemostasis system take place at the values of shear rate far exceeding those analysed in the present work[5].

Naturally, the range of thrombi-based emergency situations is far wider. Therefore a correct evaluation of the platelets' role is also of considerable interest. Attempts to develop relevant mathematical models had taken place several times [43–51]. However, for the moment only a description of platelet aggregation processes in small intensity flows ($Re \ll 1$)[6] can be considered as more or less successful [47–50].

The main distinctive feature of the model presented and employed in this work (in contrast to the ones in earlier works [52–60]) is that it takes into the consideration the dependence of the vessel wall permeability on the shear stress in intense blood flow. It seems that such effects have been mathematically described for the first time.

Another important feature of the model suggested is the introduction of the dependence of kinetic parameters (b_p, D_f, α_p) on the statistical moments M_1 and M_2 that characterize the development of fibrin polymerization processes during blood coagulation. The expressions used in the work are of an asymptotic nature. They were drawn from the application of scaling approaches [34] and the technique of composite asymptotic expansions [61] to the description of the processes of fibrin polymerization in the processes of mass transport.

In this work we neglected the change of blood viscosity during thrombi formation. Proper assessment of the role of viscoelastic rheological effects [62] in the process of intravascular thrombi formation is a task for further research work in this field.

Numerical calculations have shown that in the framework of presented boundary conditions the formation of fibre-like structures in the post-stenotic area always precedes the development of massive voluminous clot formation processes. The fibre-like structures always started to grow from the reattachment point of the recirculation zone (see fig. 2-4). That is, the nucleation center of macroscopic thrombus formation is determined by the topologic properties of the flow.

The obtained results show that the growth of fibrin fibres may lead either to the formation of localized thrombi (see fig. 2 and 3) or to the formation of friable fibrin polymer structures flattering in the flow (see fig. 4). Localized thrombi formation normally takes place in less intense flows than the formation of floating structures. In intense flows, alongside with the formation of floating structures, the formation and spreading downstream the flow of multiple fibrin microemboli takes place. It seems that such finely dispersed "dust" may

[5] In the present work, the inequation $\dot{\gamma} \leq 10^3\ s^{-1}$ was valid at all times.

[6] In the so-called Stokes approximation.

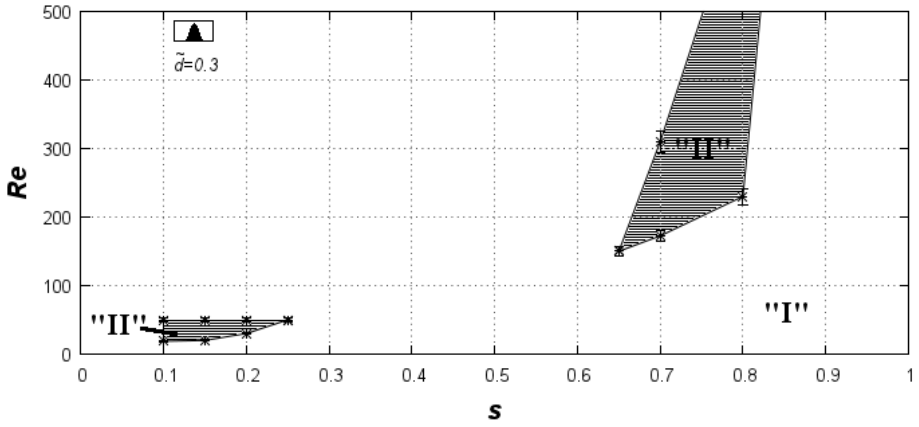

a

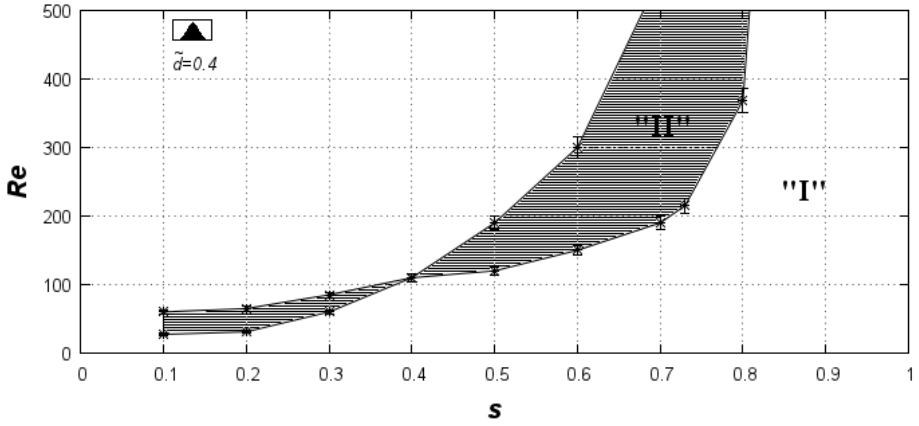

b

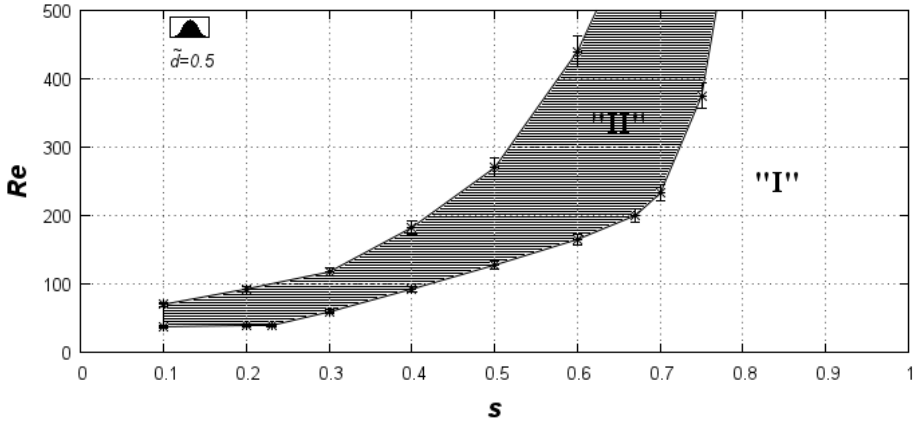

c

Figure 6: Sections of blood coagulation stability surface by the planes $\tilde{d} = const$ in the $(s, Re, \tilde{d})$ space, $\tilde{\mu}_2 = 19$. a: $\tilde{d} = 0.3$, b: $\tilde{d} = 0.4$, c: $\tilde{d} = 0.5$.

cause blood microcirculation disorders in organs situated more distally from the observed thrombi formation center.

In view of the notions listed above, it becomes clear why friable structures can be observed in the area adjacent to the right border of the "tongue" of blood liquid state stability loss (see fig. 5).

It is worth mention that the existence of some dependence of the threshold of coagulation system activation on the form of the plaque seems natural. At the same time, the character of that dependence obtained in the present work seems contrintuitive. In fact, the performed numerical calculations have shown (see fig. 6) that the plaques most dangerous with respect to thrombus formation are not the largest ones. The analysis of this phenomenon has shown that at high degrees of stenosis ($s < 0.3$) the effect of convective diminishing of procoagulants concentration may dominate over the effect of vessel wall permeability increase. The higher stenosis values ($s < 0.1$) may cause substantional changes in the flow topology, leading to a suppression of thrombus formation as well.

According to our calculations, the most thrombogenic plaques should occlude only 20-40% of the vessel lumen ($0.6 < s < 0.8$). In the light of the result it seems that the "worldwide-accepted values" that serve as indications for stenting vessels of patients exposed to atherothrombosis risk should be critically re-assessed [63–65].

The present work was partially supported by ISTC grant #3744.

References

[1] K. P. Rentrop. Thrombi in acute coronary syndromes: Revisited and revised. *Circulation*, 101:1619–1626, 2000.

[2] V. Fuster, J. J. Badimon, and J. H. Chesebro. Atherothrombosis: mechanisms and clinical therapeutic approaches. *Vasc Med*, 3:231–239, 1998.

[3] Z. M. Ruggeri. Platelets in atherothrombosis. *Nature Medicine*, 8(11):1227–1234, 2002.

[4] M. J. Davies. The pathophysiology of acute coronary syndromes. *Heart*, 83:361–366, 2000.

[5] V. W. M. van Hinsbergh. Endothelium — role in regulation of coagulation and inflammation. *Semin Immunopathol*, 34:93–106, 2012.

[6] L. Badimon, R. F. Storey, and G. Vilahur. Update on lipids, inflammation and atherothrombosis. *Thrombosis and Haemostasis*, 105 (Suppl 1):S34–S42, 2011.

[7] U. Sadat, Z. Teng, and J. H. Gillard. Biomechanical structural stresses of atherosclerotic plaques. *Expert Rev. Cardiovasc. Ther.*, 8(10):1469–1481, 2010.

[8] G. C. Makris, A. N. Nicolaides, X. Y. Xu, and G. Geroulakos. Introduction to the biomechanics of carotid plaque pathogenesis and rupture: review of the clinical evidence. *The British Journal of Radiology*, 83:729–735, 2010.

[9] V. P. Shirinskii. The role of light-chain myosin kinase in endothelial barrier functions and the prospects for use of its inhibitors in impaired vascular permeability. *Cardiologichesky vestnik*, 1(XIII):39–42, 2006.

[10] K. K. Wu and P. Thiagarajan. Role of endothelium in thrombosis and hemostasis. *Annu. Rev. Med.*, 47:315–331, 1996.

[11] P. K. Shah. Inflammation and plaque vulnerability. *Cardiovasc Drugs Ther*, 23:31–40, 2009.

[12] Z. M. Ruggeri. Mechanisms of shear-induced platelet adhesion and aggregation. *Thromb. Haemost.*, 70(1):119–123, 1993.

[13] B. R. Alevriadou, J. L. Moake, N. A. Turner, Z. M. Ruggeri, B. J. Folie, M. D. Phillips, A. B. Schreiber, M. E. Hrinda, and L. V. McIntire. Real-time analysis of shear-dependent thrombus formation and its blockade by inhibitors of von Willebrand factor binding to platelets. *Blood*, 81(5):1263–1276, 1993.

[14] Z. M. Ruggeri, J. N. Orje, R. Habermann, A. B. Federici, and A. J. Reininger. Activation-independent platelet adhesion and aggregation under elevated shear stress. *Blood*, 108:1903–1910, 2006.

[15] J. M. Tarbell. Shear stress and the endothelial transport barrier. *Cardiovascular Research*, 87(2):320–330, July 15 2010.

[16] C. J. Slager, J. J. Wentzel, F. J. H. Gijsen, A. Thury, A. C. van der Wal, J. A. Schaar, and P. W. Serruys. The role of shear stress in the destabilization of vulnerable plaques and related therapeutic implications. *Nat Clin Pract Cardiovasc Med*, 2(9):456–464, 2005.

[17] Y. Fukumoto, T. Hiro, T. Fujii, G. Hashimoto, T. Fujimura, J. Yamada, T. Okamura, and M. Matsuzaki. Localized elevation of shear stress is related to coronary plaque rupture. *JACC*, 51(6):645–650, 2008.

[18] S. D. Gertz and W. C. Roberts. Hemodynamic shear force in rupture of coronary arterial atherosclerotic plaques. *The American Journal Of Cardiology*, 66:1368–1372, 1990.

[19] R. Ross. Atherosclerosis — an inflammatory disease. *N. Engl. J. Med.*, 340:115–126, 1999.

[20] M. T. Davies. Stability and instability two faces of coronary atherosclerosis. *Circulation*, 90:2013–2019, 1994.

[21] G. Th. Guria, M. A. Herrero, and K. E. Zlobina. A mathematical model of blood coagulation induced by activation sources. *Discr Cont Dyn Syst A*, 25(1):175–194, 2009.

[22] G. T. Guria, M. A. Herrero, and K. E. Zlobina. Ultrasound detection of externally induced microthrombi cloud formation: a theoretical study. *Journal of Engineering Mathematics*, 66(1-3):293–310, 2010.

[23] A. S. Rukhlenko, O. A. Dudchenko, K. E. Zlobina, and G. Th. Guria. Threshold activation of blood coagulation as a result of elevated wall shear stress. *Proceedings of MIPT*, 4(2):192–201, 2012.

[24] A. S. Rukhlenko, K. E. Zlobina, and G. Th. Guria. Hydrodynamical activation of blood coagulation in stenosed vessels. Theoretical analysis. *Computer Research and Modeling*, 4(1):155–183, 2012.

[25] A. S. Rukhlenko. *Mathematical modeling of thrombus formation processes in intensive blood flow conditions*. PhD thesis, MIPT, Dolgoprudny, 2013.

[26] F. I. Ataullakhanov and G. T. Guria. Spatial aspects of human blood clotting dynamics I. Hypothesis. *Biophysics*, 39(1):89–96, 1994.

[27] F. I. Ataullakhanov, G. T. Guria, and A. YU. Safroshkina. Spatial aspects of human blood clotting dynamics II. Phenomenological model. *Biophysics*, 39(1):97–104, 1994.

[28] M. V. Volkenstein. *Molecular biophysics*. Academic press, New York, 1977.

[29] G. Strobl. *The Physics of Polymers. Concepts for Understanding Their Structures and Behavior*. Springer-Verlag Berlin Heidelberg, 3rd edition, 2007.

[30] S. K. Friedlander. *Smoke, Dust, and Haze: Fundamentals of Aerosol Dynamics*. Oxford, 2000.

[31] S. Uzlova, K. Guria, and G.Th. Guria. Acoustic determination of early stages of intravascular blood coagulation. *Philos Trans R Soc A*, 366:3649–3661, 2008.

[32] S. G. Uzlova, K. G. Guria, A. A. Shevelev, S. A. Vasiliev, and G.Th. Guria. Acoustically detectable intravascular microemboli as precursors of postoperative complications. *Bulletin of Bakoulev Scientific Center for Cardiovascular Surgery*, (6):55–64, 2008. In Russian.

[33] M. Doi and S. F. Edwards. *The Theory of Polymer Dynamics*. International series of monographs on physics. Oxford University Press, 1988.

[34] P. G. de Gennes. *Scaling Concepts in Polymer Physics*. G - Reference, Information and Interdisciplinary Subjects Series. Cornell University Press, 1979.

[35] M. A. Herrero. Mathematical models of aggregation: the role of explicit solutions. *Progress in nonlinear differential equations and their applications*, 63:309–318, 2005.

[36] R. F. Schmidt and G. Thews. *Human Physiology*. Springer-Verlag, New York, 1989.

[37] John W. Weisel. Fibrinogen and fibrin. In David A. D. Parry and John M. Squire, editors, *Fibrous Proteins: Coiled-Coils, Collagen and Elastomers*, volume 70 of *Advances in Protein Chemistry*, pages 247–299. Academic Press, 2005.

[38] L. Bachmann, W. W. Schmittfumian, R. Hammel, and K. Lederer. Size and shape of fibrinogen. 1. electron-microscopy of hydrated molecule. *Makromol Chem-Macromol Chem Phys*, 176(9):2603–2618, 1975.

[39] Tobias Saam, Jianming Cai, Lin Ma, You-Quan Cai, Marina S. Ferguson, Nayak L. Polissar, Thomas S. Hatsukami, and Chun Yuan. Comparison of symptomatic and asymptomatic atherosclerotic carotid plaque features with in vivo mr imaging. *Radiology*, 240(2):464–472, August 2006.

[40] Y. Sato, K. Hatakeyama, K. Marutsuka, and Y. Asada. Incidence of asymptomatic coronary thrombosis and plaque disruption: comparison of non-cardiac and cardiac deaths among autopsy cases. *Thromb Res*, 124(1):19–23, May 2009.

[41] I. M. Lifshitz and V. V. Slyozov. The kinetics of precipitation from supersaturated solid solutions. *J. Phys. Chem. Solids*, 19:35–50, 1961.

[42] V. V. Slezov. *Kinetics of First-Order Phase Transitions*. John Wiley & Sons, 2009.

[43] D. M. Wootton, C. P. Markou, S. R. Hanson, and D. N. Ku. A mechanistic model of acute platelet accumulation in thrombogenic stenoses. *Annals of Biomedical Engineering*, 29:321–329, 2001.

[44] B. J. Folie and L. V. Mcintire. Mathematical analysis of mural thrombogenesis. concentration profiles of platelet-activating agents and effects of viscous shear flow. *Biophysical Journal*, 56:1121–1141, 1989.

[45] Z. Xu, N. Chen, M. M. Kamocka, E. D. Rosen, and M. Alber. A multiscale model of thrombus development. *J. R. Soc. Interface*, 5:705–722, 2008.

[46] C. Q. Xu, Y. J. Zeng, and H. Gregersen. Dynamic model of the role of platelets in the blood coagulation system. *Medical Engineering & Physics*, 24:587–593, 2002.

[47] A. L. Fogelson and R. D. Guy. Platelet-wall interactions in continuum models of platelet thrombosis: formulation and numerical solution. *Mathematical Medicine and Biology*, 21:293–334, 2004.

[48] A. L. Fogelson and R. D. Guy. Immersed-boundary-type models of intravascular platelet aggregation. *Comput. Methods Appl. Mech. Engrg.*, 2007.

[49] A. L. Kuharsky and A. L. Fogelson. Surface-mediated control of blood coagulation: The role of binding site densities and platelet deposition. *Biophysical Journal*, 80:1050–1074, 2001.

[50] K. Leiderman and A. L. Fogelson. Grow with the flow: a spatial-temporal model of platelet deposition and blood coagulation under flow. *Mathematical Medicine and Biology*, 28(1):47–84, 2011.

[51] S. L. Diamond, J. Purvis, M. Chatterjee, and M. H. Flamm. Systems biology of platelet-vessel wall interactions. *Frontiers in Physiology*, 4:1–9, 2013.

[52] R. D. Guy, A. L. Fogelson, and J. P. Keener. Fibrin gel formation in a shear flow. *Math. Med. Biol.*, 24(1):111–130, 2007.

[53] A. P. Guzevatykh, A. I. Lobanov, and G. Th. Guria. Thershold intervascular blood coagulation as a result of stenosis development. *Mathematical modeling*, 12(4):39–60, 200.

[54] A. L. Chulichkov, A. V. Nikolaev, A. I. Lobanov, and G. T. Guria. Threshold activation of blood coagulation and thrombus growth under flow conditions. *Mathematical modeling*, 12(3):76–95, 2000.

[55] M. Anand, K. Rajagopal, and K. R. Rajagopal. A model incorporating some of the mechanical and biochemical factors underlying clot formation and dissolution in flowing blood. *J. of Theoretical Medicine*, 5:183–218, 2003.

[56] M. Anand, K. Rajagopal, and K. R. Rajagopal. A model for the formation and lysis of blood clots. *Pathophysiol. Haemost. Thromb.*, 34:109–120, 2005.

[57] A. I. Lobanov and T. K. Starozhilova. Effect of convective flow on formation of two-dimensional structures in the model of blood coagulation. *Phystech Journal*, 3(2):96–105, 1997.

[58] A. I. Lobanov and T. K. Starozhilova. The effect of convective flows on blood coagulation processes. *Pathophysiol Haemost Thromb*, 34:121–134, 2005.

[59] M. K. Runyon, C. J. Kastrup, B. L. Johnson-Kerner, G. Thuong, Van Ha, and R. F. Ismagilov. Effects of shear rate on propagation of blood clotting determined using microfluidics and numerical simulations. *JACS*, 130(11):3458–3464, 2008.

[60] K. B. Neeves, D. A.R. Illing, and S. L. Diamond. Thrombin flux and wall shear rate regulate fibrin fiber deposition state during polymerization under flow. *Biophysical Journal*, 98(7):1344–1352, 2010.

[61] A. H. Nayfeh. *Perturbation Methods*. Physics textbook. Wiley, 2008.

[62] A. Ya. Malkin. The state of the art in the rheology of polymers: Achievements and challenges. *Polymer Science, Ser. A*, 51(1):80–102, 2009.

[63] E. Eeckhout et al. Indications for intracoronary stent placement: the European view. *European Heart Journal*, 20(14):1014–1019, 1999.

[64] Bates et al. ACCF/SCAI/SVMB/SIR/ASITN 2007 Clinical Expert Consensus Document on Carotid Stenting. *Journal of the American College of Cardiology*, 49(1):126–170, 2007.

[65] Patel et al. ACCF/SCAI/STS/AATS/AHA/ASNC/HFSA/SCCT 2012 Appropriate Use Criteria for Coronary Revascularization Focused Update. *Journal of the American College of Cardiology*, 59(9):857–881, 2012.